# 2. Sandstone petrology and provenance of the Chaco Basin: record of foreland basin evolution and Andean uplift

CAROLA HULKA[1], CORNELIUS E. UBA[1], CHRISTOPH HEUBECK[1]

[1]*Freie Universität Berlin, Department of Geological Sciences, Malteserstrasse 74-100, 12249 Berlin, Germany*

*Correspondence: Carola Hulka, Department of Geological Sciences, Freie Universität Berlin. Malteserstrasse 74-100, 12249 Berlin, Germany. E-mail: chulka@zedat.fu-berlin.de*

*To be submitted to: Journal of Sedimentary Research*

**Abstract**

Tectonic conditions and drainage in the southern Bolivian Chaco foreland basin provide an excellent natural laboratory to study the composition of pre- and syntectonic sediments derived from cratons and foreland fold-thrust belts under semi-humid conditions.

The streams show changing paleocurrents pattern between the pretectonic and the syntectonic strata. The pretectonic Petaca Formation shows an east-to-west flow and the overlying Yecua Formation flows north-south. The syntectonic strata (Tariquia, Guandacay, and Emborozú formations) indicate a dominant west-to-east flow from the Central Andes toward the foreland.

The most distinctive characteristics of the recognized petrofacies and their approximate time-stratigraphic spans are: quartz-rich Petaca sandstone (Oligocene to middle Miocene), very quartz-rich Yecua sandstone (middle Miocene to late Miocene), quartz-rich Tariquia sandstone with increasing content of lithic fragments and feldspar (late Miocene), quartz-rich Guandacay sandstone with significant content of lithic fragments (Late Miocene to Pliocene), and quartz-poor Emborozú sandstone with significant content of feldspar and lithic fragments (Pliocene to recent).

## 2.1 Introduction

Work in sedimentary petrology, geochemistry, and geomorphology has led to a better understanding of the relative abundance of detrital sediment controlled by climatic, transport-related, and tectonic factors (e.g. Blatt, 1967; Dickinson and Suczek, 1979; Suttner and Basu, 1981; Mack, 1984, Bilodeau and Keith, 1986; Johnsson, 1990; Johnsson et al., 1991). These data provide quantitative standards for the interpretation of provenance and paleoclimate from clastic sediments. A particularly common association of provenance types is a combined sedimentary and low-metamorphic provenance because these rocks are commonly juxtaposed along convergent plate margins and supply large volumes of clastic sediment to retroarc and peripheral basins (Dickinson, 1970; Dickinson and Suczek, 1979).

The present study examines the composition of Cenozoic sediments from the Chaco foreland basin, Bolivia, which derive from sedimentary, metamorphic, and magmatic provenances under arid to semi-humid conditions. The Chaco Basin represents the present foreland basin

of the Central Andes in southern Bolivia and contains up to 7.5 km of pretectonic and syntectonic stratigraphic sequences (Dunn et al., 1995; Gubbels et al., 1993; Moretti et al., 1996; Uba et al., in revision). These provide detrital and temporal information on the Central Andean uplift and record orogenic propagation toward an eastern foreland and consist dominantly of sandstones, mudstones, and conglomerates, as well as minor shell hash coquinas, evaporites, and tuffs.

This study describes Cenozoic sandstone petrology and conglomerate lithology of the five Cenozoic formations making up the basin fill of the central Chaco Basin, extending from Santa Cruz in the north to the Argentinian border in the south along the easternmost anticlines of the Subandean Belt (Fig. 2.2). Specifically, this paper addresses the following questions. (1) How has the composition of the Chaco Basin sandstones varied through Cenozoic time and what do the observed changes suggest about the orogenic processes of the Central Andes? (2) What provenance domains can be distinguished by sandstone composition? (3) Can sandstone modal data help constrain the propagation history of the Central Andes? .

## 2.1.1 Methods

Modal analysis of petrographic composition constitutes the basis for our subsequent sandstone classification and provenance analysis. Macroscopic field description was followed by thin sectioning of selected sandstone samples and petrographic study using a polarizing microscope. The conglomerate and mudstone classification was done by visual inspection in the field. Hulka et al. (in press) describe the composition of the rare shell hash coquinas in the Yecua Formation in detail.

Modal sandstone compositions from the Petaca, Yecua, Tariquia, Guandacay, and Emborozú Formations followed the Gazzi-Dickinson method (Gazzi, 1966; Dickinson, 1970; Ingersoll et al., 1984). In each thin section, we counted 300 framework grains. We assigned grains < 0.03 mm to matrix, following the convention of Pettijohn (1975). Tab. 2.1 summarizes the recognized grain types and their definitions.

Tab. 2.1: Framework grains

| Abbreviation | Explanation |
|---|---|
| Q | quartz, including monocrystalline and polycrystalline quartz grains |
| Qm | monocrystalline quartz |
| Qp | polycrystalline quartz, including chert |
| F | feldspar, including potassic feldspar and plagioclase |
| Fk | potassic feldspar |
| Fp | plagioclase feldspar |
| L | lithic components, including sedimentary, metasedimentary and volcanic lithic components |
| Lv | volcanic lithic components |
| Ls | sedimentary and metasedimentary lithic components |
| Lt | total lithic components, including sedimentary and metasedimentary components, volcanic components, polycrystalline quartz, and chert |

Ternary diagrams with quartz-feldspar-lithic fragments (Q-F-L) end members typically illustrate sandstone classification based on framework composition and matrix proportion. Subsidiary diagrams focus on subsets of these three principal components, e.g. after Folk (1974).

Provenance is at its most effective by using a combination of several ternary diagrams rather than relying on a single diagram because combinations of specific end members discriminate between different grain properties. A standard combination, after Dickinson and Suczek (1979), includes Q-F-L, Qm-F-Lt, Qp-Lv-Ls, and Qm-Fk-Fp diagrams (Fig. 2.1).

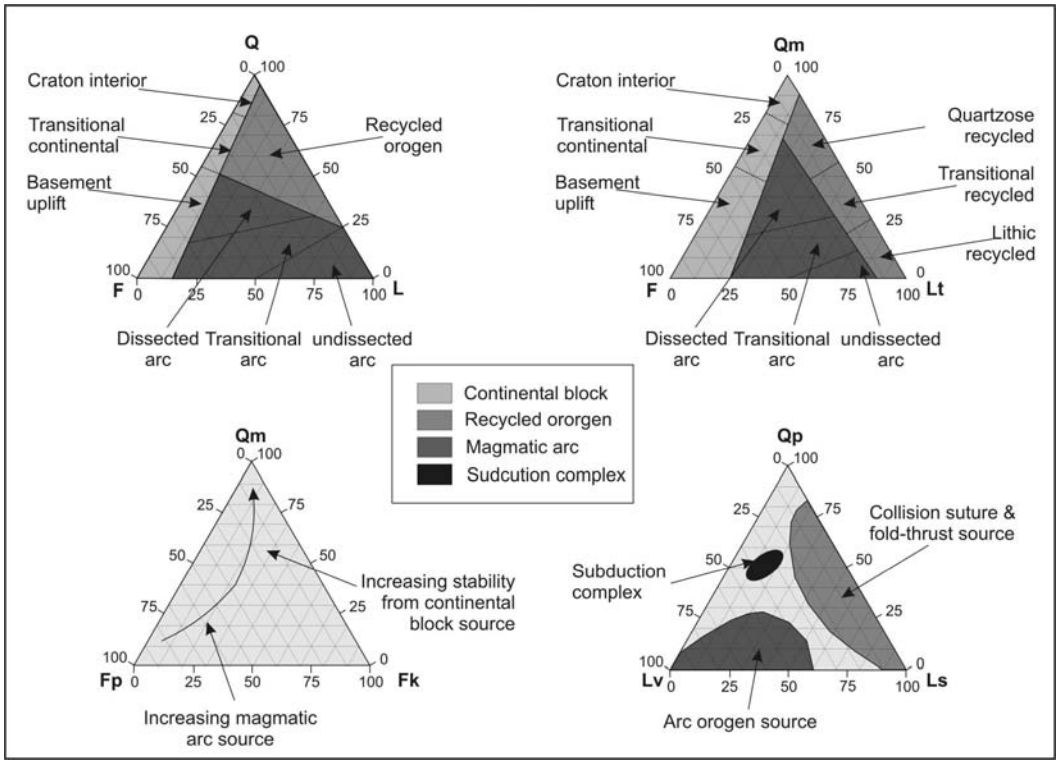


Fig. 2.1: Provenance diagrams after Dickinson and Suczek (1979)

The Q-F-L plot describes relative grain stability and weathering processes of the three end members. Therefore, this diagram may indicate transport mechanisms and source rocks.

The Qm-F-Lt plot includes the polycrystalline quartz and chert fragments (Qp) in the total lithic fragment (Lt) end member. This diagram takes in account the source rock grain size.

The Qm-Fk-Fp plot excludes the total lithic fragments (Lt) and proportionate feldspars in potassium feldspar (Fk) and plagioclase (Fp). This plot may differentiate between continent-derived, Fk-rich source rocks versus Fp-rich sources of a magmatic arc.

Finally, the Qp-Lv-Ls plot differentiates the principal lithic fragments by separating them in sedimentary and metasedimentary lithic fragment (Ls), volcanic lithic fragment (Lv) and polycrystalline quartz and chert fragments (Qp). It therefore distinguishes effectively between subduction-related source rocks, collision suture and fold-thrust-belt sources, and arc orogen sources.

## 2.1.2 Data set

Sedimentary strata composing the Chaco Basin fill are deformed and exposed best in the frontal zone of the Subandean Belt, an active, eastward-propagating classical fold-thrust belt forming the easternmost deformed structural domain of the Central Andean orogen (Sempere et al., 1990; Dunn et al., 1995; Moretti et al., 1996; Kley, 1996). Fig. 2.2 illustrates the setting of the sample location.

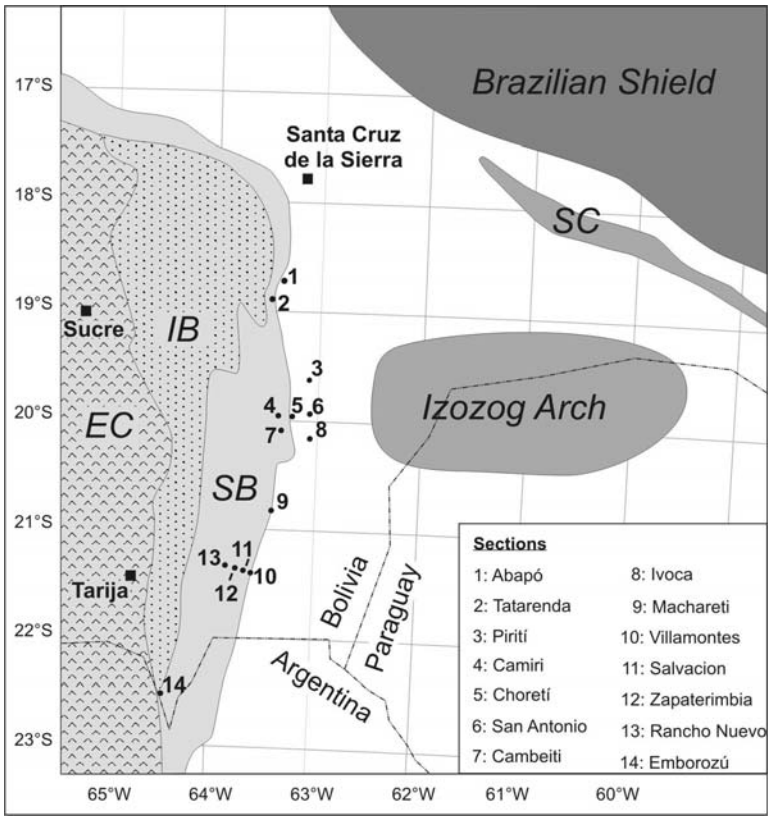


Fig. 2.2: Basemap of the northern part of the Chaco Basin, illustrating the studied sections along the western margin of the Subandean belts. Abbreviations: EC = Eastern Cordillera, IB = Interandean Belt, SB = Subandean Belt, SC = Sierras Chiquitanas (modified after Suárez-Soruco, 2000)

Tab. 2.2: Section names from which sandstone samples were taken for petrographic analysis. See Fig. 2.2 for locations.

| Location number | Emborozú Formation | Guandacay Formation | Tariquia Formation | Yecua Formation | Petaca Formation |
|---|---|---|---|---|---|
| 1 | Abapó | Abapó | | | |
| 2 | | Tatarenda | Tatarenda | Tatarenda | Tatarenda |
| 3 | | | Piritĺ | | Piritĺ |
| 4 | | | Camiri | | Camiri |
| 5 | | | Choretí | Choretí | Choretí |
| 6 | | | | San Antonio | San Antonio |
| 7 | | | | Cambeití | Cambeití |
| 8 | | | Ivoca | | Ivoca |
| 9 | | | Machareti | | Machareti |
| 10 | | | Villamontes | | Villamontes |
| 11 | | | Salvacion | | Salvacion |
| 12 | | | Zapaterimbia | | Zapaterimbia |
| 13 | | | Rancho Nuevo | | Rancho Nuevo |
| 14 | Emborozú | | Emborozú | | Emborozú |
| Number of samples | 6 | 4 | 25 | 7 | 30 |

## 2.2 Cenozoic Chaco Basin stratigraphy

Chaco basin fill architecture is conventionally subdivided in five formations (from base to the top): the Petaca, Yecua, Tariquia, Guandacay, and Emborozú Formations. These are principally defined through lithostratigraphic attributes (Sempere et al., 1990; Marshall and Sempere, 1991; Marshall et al., 1993; Gubbels et al., 1993; Coudert et al., 1995; Moretti et al., 1996, Jordan et al., 1997; Kley et al., 1997; Uba et al., in revision).

The up-to-100 m-thick Petaca Formation overlies a low-relief but uneven, weathered Mesozoic land surface with indistinct, possibly unconformable contact. It consists of calcretes, reworked pedogenic clasts of conglomerate size, and redbed fluvial sandstones and mudstones. This unit represents extensive pedogenesis under an arid to semiarid climate, modified by ephemeral braided streams (Uba et al., in revision; Fig. 2.3). The age of the Petaca Formation is poorly constrained by biostratigraphy. The Deseadean notohippid cf. *Rhynchippus*, found near the base of the Petaca Formation, indicates a late Oligocene-earliest Miocene age (~ 27 Ma; Marshall and Sempere, 1991; Marshall et al., 1993).

The up-to-250m-thick Yecua Formation overlies the Petaca Formation conformably. It consists of vary-colored mudstones, calcareous and quartzitic sandstones, subordinate thin shell hash coquinas, and minor ooid limestones representing restricted marginal marine environments including coastal floodplains, floodplain lacustrine environments, tidal environments, medium-energy sandy shorelines, and shallow offshore (Fig. 2.3; Hulka et al., in press). Foraminifera (Hulka et al., in press) indicate a short-lived restricted marginal-marine environment of middle to late Miocene age (14-7 Ma).

The up-to-4500m-thick Tariquia Formation overlies transitionally the Yecua Formation in the north and the Petaca Formation in the south, respectively (Uba et al, in revision). However, a new seismic interpretation of Uba (2005), also suggest a terrestrial facies of the Yecua Formation. It consists of thick, red, moderately channelised sandstones and interbedded mudstones representing anastomosing stream channels and floodplains (Fig. 2.3). Marshall and Sempere (1991) described fish fossils along the base of the Tariquia Formation of Chasicoan to Huaquerian age (late Miocene, 8-6 Ma; Moretti et al., 1996). Our biostratigraphic study (Hulka et al., in press; chapter 3) suggests that the base of the Tariquia Formation may be approximately 7 Ma old.

The up-to-1500m-thick, sandstone-dominated Guandacay Formation shows a coarsening- and thickening-upward sequence in a braided-stream environment including channelised sandstones, gravel sheets, and thin subordinate mudstones (Uba et al., in revision, Fig. 2.3). An angular discontinuity of late Miocene age (6 Ma) between the Tariquia Formation and the Guandacay Formation is visible on seismic data, for example between Villamontes and La Vertiente (Moretti et al., 1996). Marshall and Sempere (1991) described the skeleton of a notoungulate along the base of the Guandacay Formation, suggesting a Chasicoan to Huayquerian age (> 5.3 Ma).

Lastly, the up-to-1650-m-thick the Emborozú Formation represents the youngest strata within the Chaco Basin fill. This formation consists predominantly of coarsening-up cobble- and-boulder conglomerates, subordinate sandstones, and sandy mudstones, representing alluvial-fan deposits (Fig. 2.3). Moretti et al. (1996) documented a tuff within the Emborozú Formation at 3.3 Ma.

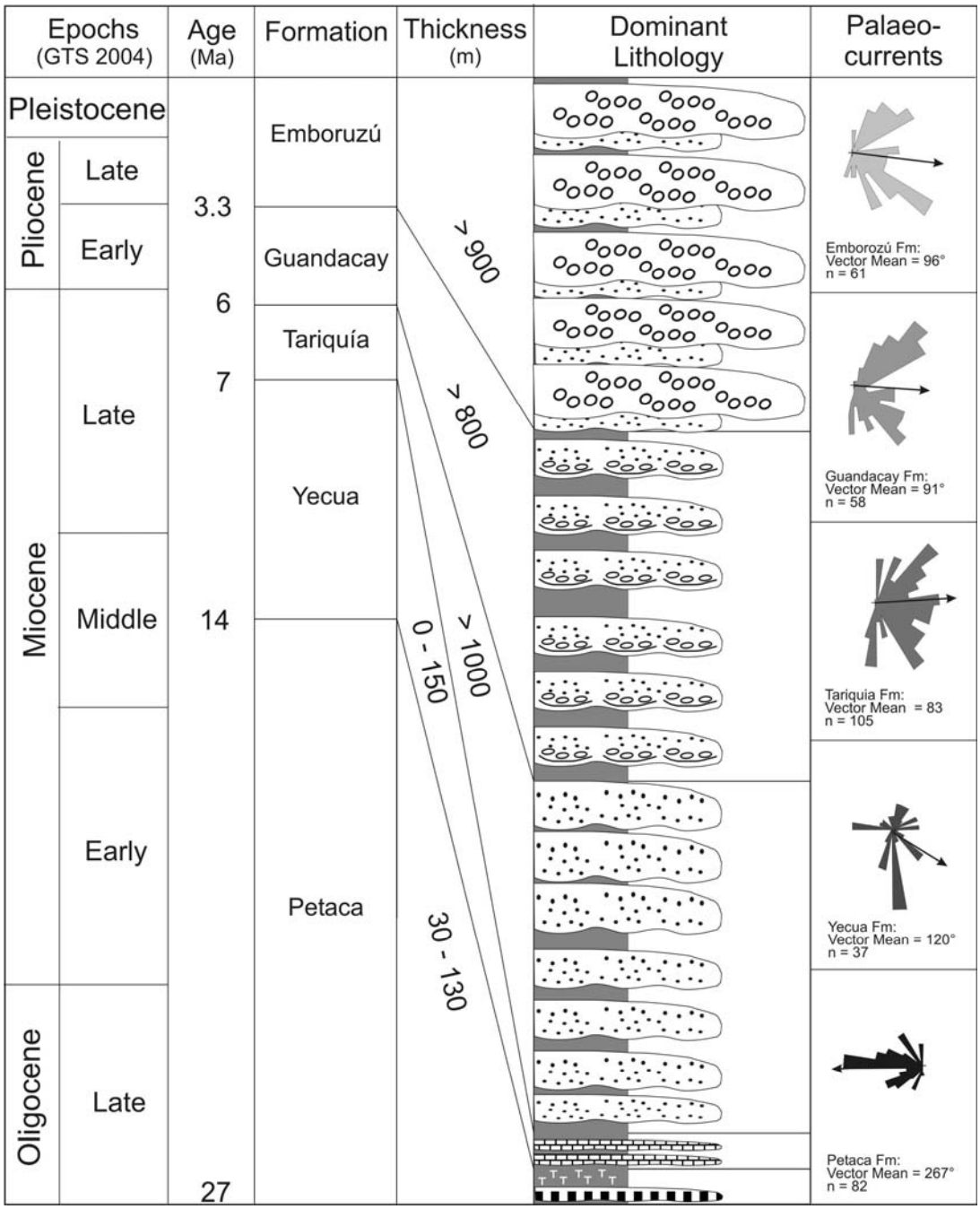


Fig. 2.3: Schematic stratigraphic columns of the Chaco Basin fill including its five Cenozoic formations: Petaca, Yecua, Tariquia, Guandacay, and Emborozú.

## 2.2.1 Paleocurrents

We measured 179 foresets of trough crossbeds, mostly in fluvial channels, throughout the western Chaco Basin from sandstones of the Emborozú, Guandacay, Tariquia, Yecua, and Petaca Formations (new data and data of Uba et al., in revision; Fig. 2.3).

Paleocurrents from the Petaca Formation indicate a dominant westward transport direction, and a bidirectional transport direction in the Yecua Formation. Average transport directions in the Tariquia, Guandacay, and Emborozú Formations are consistently eastward, with those of the Tariquia Formation exhibiting greater variability.

These data demonstrate that fluvial-alluvial deposition since the late Miocene is dominated by Andean erosion and essentially identical to the modern fluvial drainage pattern along the western margin of the basin. The higher scattering of Tariquia paleocurrents is consistent with the reduced stream power in semiarid anastomosing streams.

### 2.2.2 Volcanic components

A volumetrically minor but potentially significant component of the basin fill consists of several thin, discontinuous and poorly exposed air-fall tuffs in the Tariquia, Guandacay, and Emborozú Formations. Allmendinger et al. (1997) document voluminous ignimbrites of late Miocene and Pliocene age (3-2 Ma) from the Altiplano and Puna plateaus and its margins. Significant ignimbrites of 8-6.5 Ma age are also known from the eastern Altiplano and the western part of the Eastern Cordillera (Allmendinger et al., 1997). Coira et al. (1993) also described backarc stratovolcano-caldera complexes during that time. Since 3 Ma, Andean volcanism is dominated by andesitic to dacitic stratovolcanic-complexes and subordinate rhyodacitic ash-flow tuffs in the Western Cordillera.

## 2.3 Potential provenance

The geographic setting of the Chaco Basin suggests the following potential provenances (Fig. 2.4): (1) the uplifted backarc region of the Central Andes to the west, (2) the Brazilian Shield to the northeast, (3) the Izozog Arch to the east, and (4) along-strike sources from the Santa Barbara System to the south and the Amazon Basin to the north. Delivery of Subandean sedimentary and metasedimentary material from the west dominates the recent basin fill.

Rocks of the Brazilian Shield, including high-grade granulite and low-grade greenschists, are exposed north and northeast of the Chaco Basin. The Sierras Chiquitanas (SC in Fig. 2.4) represent a mobile belt of Late Proterozoic to Cambrian metasediments along the southeastern margin of the Brazilian Shield (Jones, 1985).

To the west, the strata of the Chaco Basin pinch out against a zone of basement uplift, the Izozog arch. This region was probably uplifted as early as the Carboniferous (Moretti et al., 1996) and represents a long-lived zone of erosion or non-deposition (from Mesozoic up to the late Miocene). Seismic data suggest that the Izozog Arch comprises sedimentary strata up to Devonian age.

During its entire history, the Chaco Basin was bordered to the west by the eastward-prograding front of the Subandean fold-thrust belt. This orogenic front presently largely recycles the western part of the Tertiary Chaco basin fill but also exposes a thick sequence of underlying Paleozoic strata in their anticlines and thrust tips, mostly of Mesozoic continental-interior environments but also including Permo-Carboniferous glacial diamictites and the Triassic Entre-Rios basalt. Deformation of the Subandean belt started not before 6 Ma (Kley, 1993; Gubbels et al., 1993; Husson and Moretti, 2002; Ege, 2004), limiting its contribution to the Chaco Basin to the Tariquia Formation and overlying strata.

The Subandean fold-thrust belt is backed up to the west, beyond a principal thrust, by the narrow Interandean Belt, which presently exposes mostly Devonian/Silurian sedimentary strata (Kley, 1996; Müller et al., 2002), with small remnants of Carboniferous strata. The composition and thickness of formerly overlying, now-eroded strata is speculative. The Interandean Belt may have formed a potential source area for westerly-derived sediments to

the Chaco since the middle Miocene. The Eastern Cordillera, in turn west of the Interandean zone, has been uplifted and eroded since the late Oligocene and therefore may have contributed to the Chaco basin fill since that time. It principally consists of > 8 km thick Ordovician sandstones (Erdtmann et al., 1995; Jacobshagen et al., 2002). Kley and Reinhardt (1994) concluded that the Ordovician rocks were overlain by 4-6 km of Paleozoic sediments which in turn were unconformably overlain by up to 2500 m of Cretaceous and Paleogene sandstones, mudstones, and subordinate lacustrine carbonates and pedogenically-altered mudstones (Kley, 1996; DeCelles and Horton, 2003; Fig. 2.5).

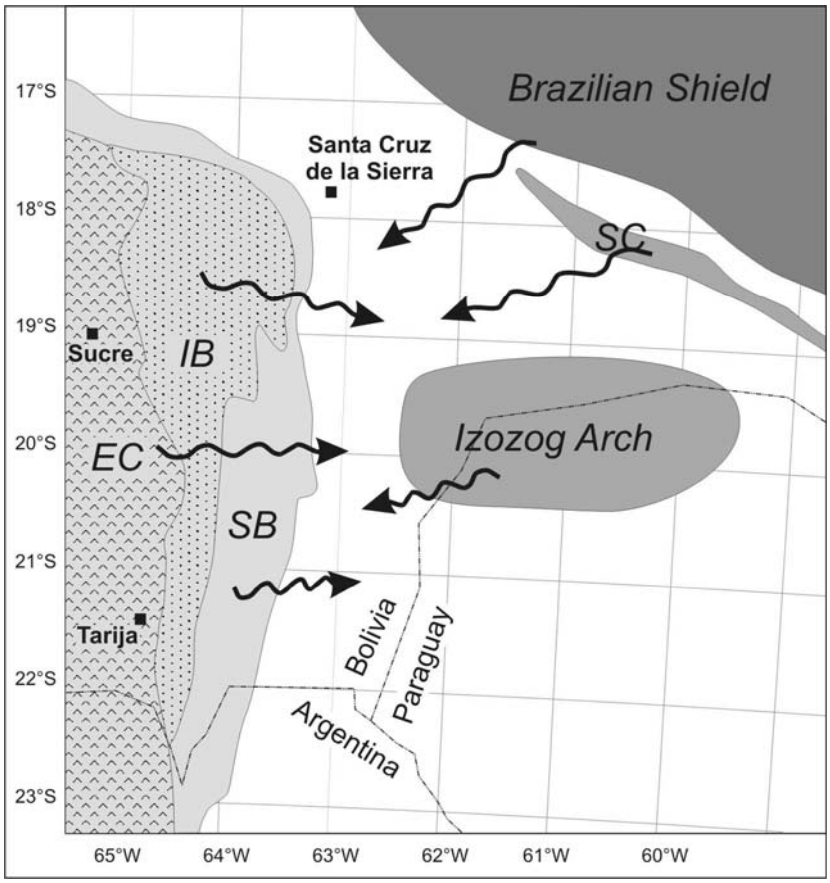


Fig. 2.4: Map showing the surrounding geological provinces (after Suárez-Soruco, 2000), which may be source areas for the Cenozoic sediments. Abbreviations: EC = Eastern Cordillera, IB = Interandean Belt, SB = Subandean Belt, SC = Sierras Chiquitanas

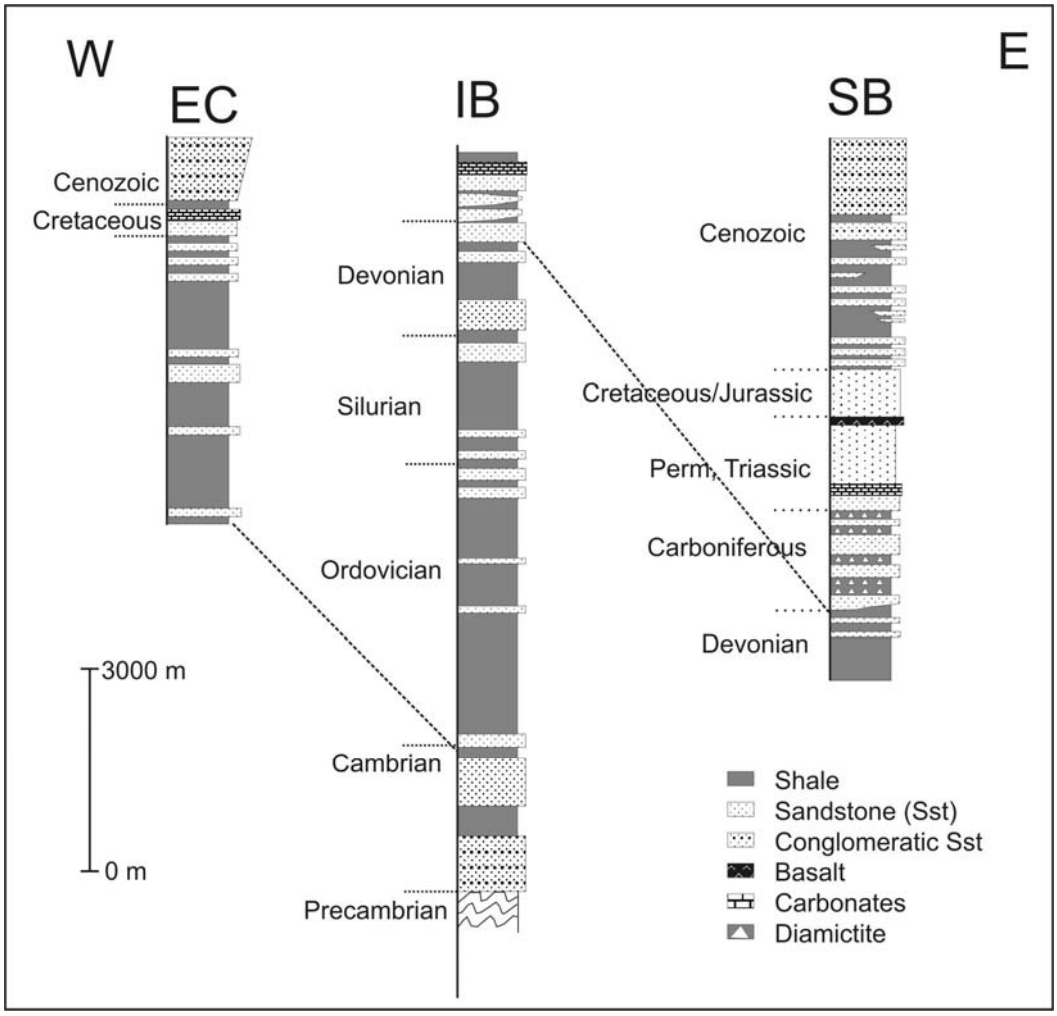


Fig. 2.5: Stratigraphic columns of the backarc region of the Central Andes for the Eastern Cordillera (DeCelles and Horton, 2003), the Interandean Belt, and the Subandean belt (after Kley, 1996)

Initial uplift and exhumation started in the central Eastern Cordillera in the late Eocene (approximately 42 Ma) and propagated since the Oligocene (approximately 32 Ma) to the eastern part of the Eastern Cordillera (Fig. 2.6; Ege et al., in preparation). The exhumation front was situated in early Miocene (18 Ma) in the central Interandean belt and reached the western Subandean belt in the late Miocene (between 11 and 8 Ma; Ege et al., in preparation). Probably, the eastern part of the Subandean belt was not affected by exhumation before 6 Ma (latest late Miocene).

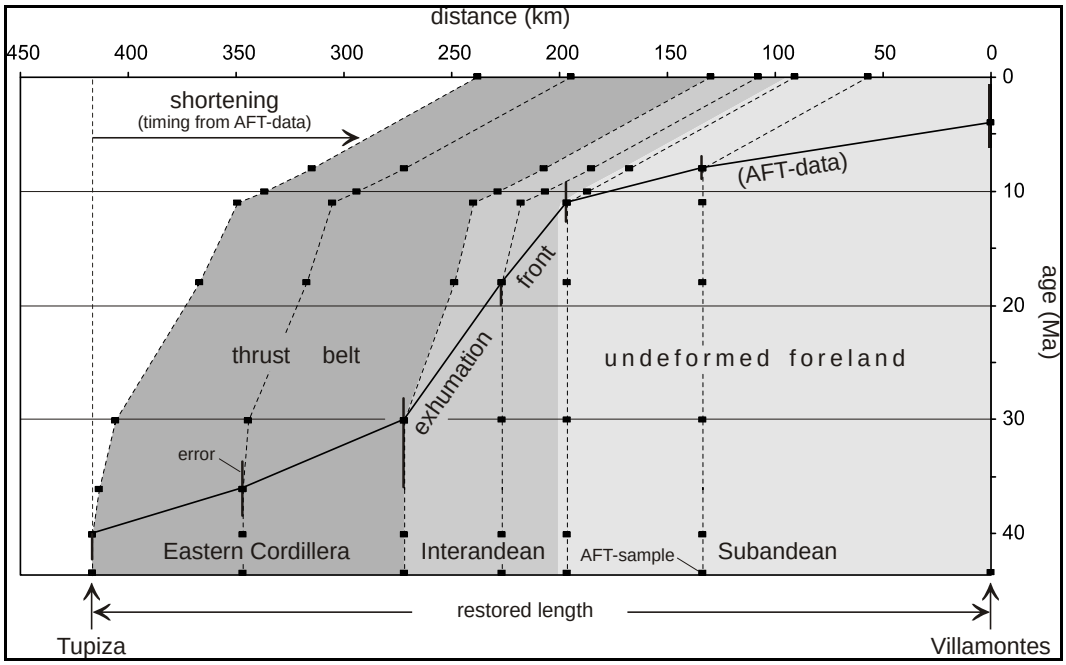


Fig. 2.6: Eastward propagation of the exhumation front (solid line) between the central Eastern Cordillera and the eastern Subandean inferred from interpretation of cooling ages (Ege et al., in preparation). The stippled curves represent the eastward displacement of the sample locations from cumulated shortening values (Dunn et al., 1995; Kley, 1996; Müller et al., 2002).

# 2.4 Results

## 2.4.1 Conglomerate composition

Conglomerates allow more specific lithological provenance identification than sandstones but their occurrence is strongly limited by transport mechanisms. Conglomerate stringers occur in the Petaca Formation, are absent from the Yecua (except for intrabasinal material) and Tariquia Formations, and become dominant in the Guandacay and Emborozú Formation.

In the Petaca Formation, pebble conglomerates in up to 50 cm thick, lateral continuous beds represent reworked, locally derived underlying pedogenic horizons and therefore contain mainly calcrete- and silcrete-clasts (Fig. 2.7). Calcrete clasts are mostly moderate to well rounded whereas the more resistant silcrete clasts are sub- to medium-rounded.

Conglomerates of the Guandacay Formation consist of oligomictic metaquartzites, which are generally matrix-supported, subangular to subrounded (Fig. 2.7) and occur in sheet-like units of maximum 10 m thickness (Uba et al., in revision). Individual clasts are usually 3 to 5 cm in diameter but can reach up to 10 cm. The source of the conglomerates probably consists of Ordovician and Mesozoic sandstones and quartzites from the adjacent backarc of the Central Andes (Uba et al., in revision).

Conglomerates of the Emborozú Formation reach several m thick and are generally clast-supported, and rounded to very rounded (Fig. 2.7). Clasts show a median diameter of approx. 15 cm. Imbrication is common. Uba et al. (in revision) list Ordovician, Devonian and Cretaceous sedimentary to metasedimentary source rocks of the Subandean and Interandean belt.

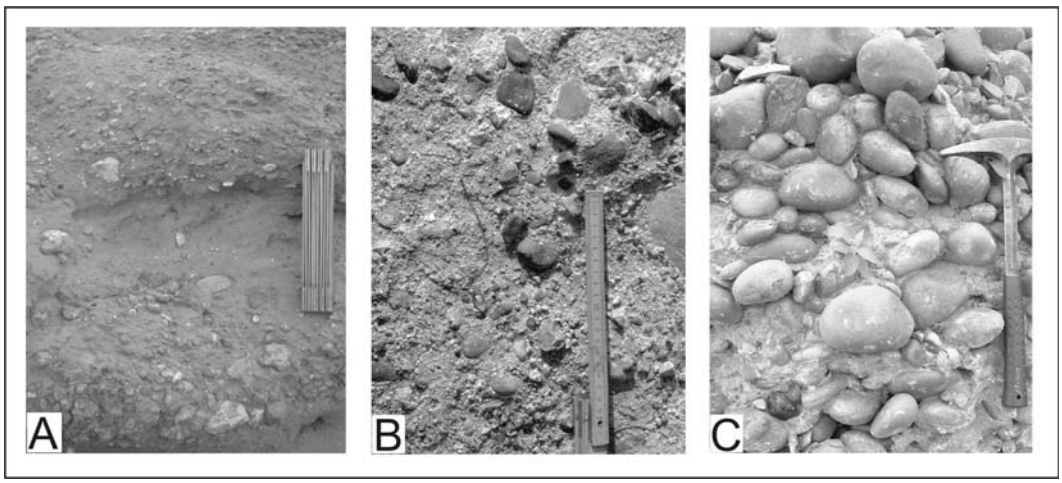


Fig. 2.7: Conglomerates of the Petaca Formation at the base of Iguamirante section (A), of the Guandacay Formation in Abapó section (B), and of the Emborozú Formation near the top of Abapó section (hammer is 55 cm long).

## 2.4.2 Grain categories of the sandy material

The following paragraph briefly describes the major grain components of Petaca, Yecua, Tariquia, Guandacay, and Emborozú Formations sandstones. Results of thin section point counts are listed in Appendix C.

### Quartz

Quartz constitutes the highest proportion in all sandstone samples. Monocrystalline quartz grains are rounded to very well rounded. Sorting ranges from very poor to very good. More than 60 % of the monocrystalline quartz grains show undulatory extinction; many quartz grains show inclusions (Fig. 2.8A). The proportion of polycrystalline quartz grains is generally lower than that of monocrystalline quartz (Fig. 2.8B). Domain boundaries may be straight or sutured. Fine- or coarse-sand-grained cherts as well as microcrystalline grains are rare to common.

### Feldspar

Feldspars are well preserved and angular to rounded. Corrosion by sericitication is common within coarse-grained crystals. Polysynthetic plagioclase twins are common (Fig. 2.8C). The grains of the potassic feldspars are untwinned, show Carlsbad twinning or distinctive Microcline twinning. Perthite intergrowth of plagioclase into potassic feldspar is common (Fig. 2.8D).

### Lithic fragments (L)

Lithic fragments are subdivided into magmatic lithic fragments (Lv) delivered from magmatic sources, sedimentary lithic fragments (Ls) from sedimentary source rocks, and metamorphic lithic fragments, including metasedimentary and metavolcanic rocks. We counted the metasedimentary grains as Ls; metavolcanic grains as Lv.

Plutonic-sourced lithic fragments are conspicuous through their absence. Volcanic fragments are coarse- and very-coarse-grained and in general well rounded. They contain microphenocrysts of quartz, biotite, and plagioclase in a groundmass of fine-grained feldspar, pyroxene, and opaque minerals (Fig. 2.8E).

The few thin sections with substantial content of volcanic fragments show mostly granular felsitic grains with mainly anhedral microcrystalline quartz and feldspar, suggesting an intermediate composition of its source rock. Lathwork, microlitic, and vitric grain types are absent. The occurrence of a balanced plagioclase-potassium feldspar ratio and of quartz phenocrysts suggests an overall dacitic, rather than andesitic contribution. Therefore, we suggest that the volcanic material largely derived from dacitic stratovolcano complexes of the Central Andes backarc region.

Lithic sedimentary grains include siliciclastic fragments and carbonate grains. Carbonate grains occur within the Yecua Formation as intrabasinal ooid and reworked shell fragments. Siliciclastic grains are composed of sand-sized shale clasts, which include quartz and feldspar grains in a clayey groundmass (Fig. 2.8F, G).

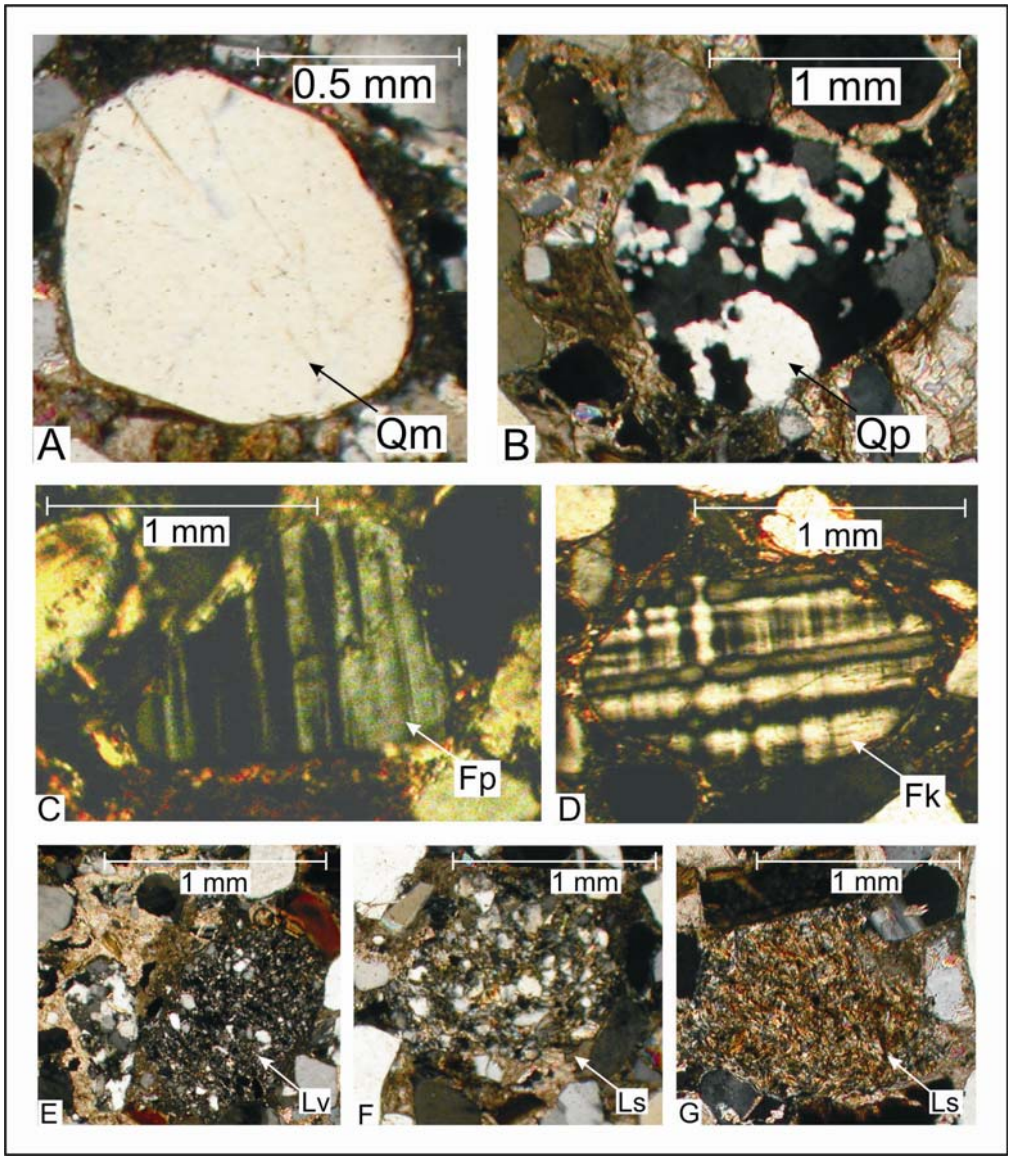


Fig. 2.8: Thin-section photomicrographs of representative major framework grains from sandstones of the Chaco Basin. (A) Monocrystalline veined quartz (Qm) of the Yecua Formation (San Antonio section). (B) Polycrystalline quartz (Qp) of the Yecua Formation (San Antonio section). (C) Plagioclase (Fp) of the Tariquia Formation (Camiri section). (D) Microcline (Fk) of the Tariquia Formation (Camiri section). (E) Lithic volcanic granular felsitic grain (Lv) of the Tariquia Formation (Camiri section). (F) fine-grained sandstone grain (Ls) of the Tariquia Formation (Camiri section). (G) Metasedimentary lithic fragments (Ls) of the Emborozú Formation (Abapó section). For locations, see Fig. 2.2.

### Accessory minerals

Sand-sized micas are a minor constituent in the Tariquia, Guandacay, and Emborozú Formations. Biotite outweighs white micas. Opaque minerals and heavy minerals are rare.

### Matrix

Matrix is composed of clay minerals and ranges between 5 and 10 % in the Petaca Formation and Yecua Formation but lower, ca. 5%, within the Tariquia, Guandacay, and Emborozú formations. The high interference colors suggest high smectite content.

### Cement

Quartz, calcite, and clay cementation are common within the Petaca Formation with minor chalcedonic cementation. Calcite is the most common cement within the Yecua Formation, with subordinate quartz cement. Clay cement dominates in the Tariquia, Guandacay and Emborozú Formations with subordinate quartz cementation. We do not observe calcitic cement in the studied samples.

## 2.4.3 Sandstone classification

Sandstones of the Petaca and Yecua Formations are quartzarenites and quartz-rich subarkoses; only one sample of the Yecua Formation is a sublitharenite (Fig. 2.9). Monocrystalline quartz dominates the quartz fraction. The feldspar fraction is almost equally balanced between potassic and plagioclase feldspar. Lithic fragments contain nearly exclusively sedimentary and metasedimentary fragments, mostly consisting of reworked mudstone grains.

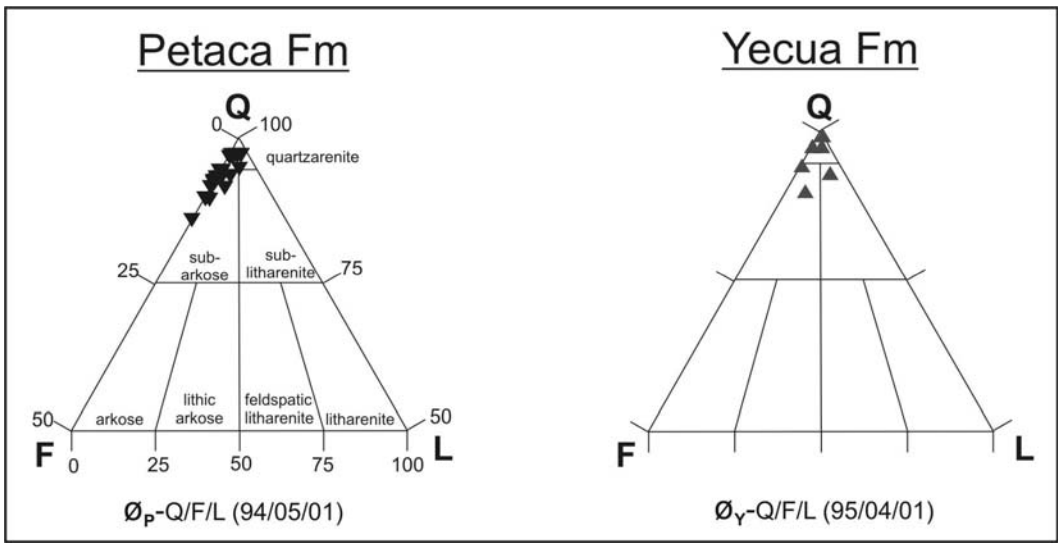


Fig. 2.9: Sandstone classification of the Petaca Formation (Fm) and the Yecua Formation (Fm).

The sandstone composition of the Tariquia Formation varies and includes mainly sublitharenites to quartz-rich subarkoses (Fig. 2.10). The quartz fraction is dominated by monocrystalline quartz. The content of plagioclase and alkali feldspar is balanced. Polycrystalline quartz dominates the lithic fraction and contains a significant proportion of (meta-) sedimentary lithic fragments.

The samples of the Guandacay Formation are from two outcrops of the northern part of the Chaco Basin. All four samples represent sublitharenites (Fig. 2.10). The quartz fraction is

dominated by monocrystalline quartz; plagioclase and alkali feldspar is balanced. The lithic fraction is dominated by polycrystalline quartz and contains a large proportion of (meta-) sedimentary lithic fragments.

Samples of the Emborozú Formation were studied in only two sections, one each from the northern and the southern part of the basin. The sandstones are litharenites (Fig. 2.10). The quartz fraction is dominated by monocrystalline quartz. The content of plagioclase and alkali feldspar is balanced, and the lithic fraction is dominated by polycrystalline quartz and (meta-) sedimentary lithic fragments.

Fresh outcrops of Emborozú Formation sandstones are rare. Six sandstones from two sections are litharenites, except one sample of lithic-arkose composition (Fig. 2.10). The quartz fraction is dominated by monocrystalline quartz. The content of plagioclase and alkali feldspar is balanced, and the lithic fraction is dominated by polycrystalline quartz and (meta-) sedimentary lithic fragments.

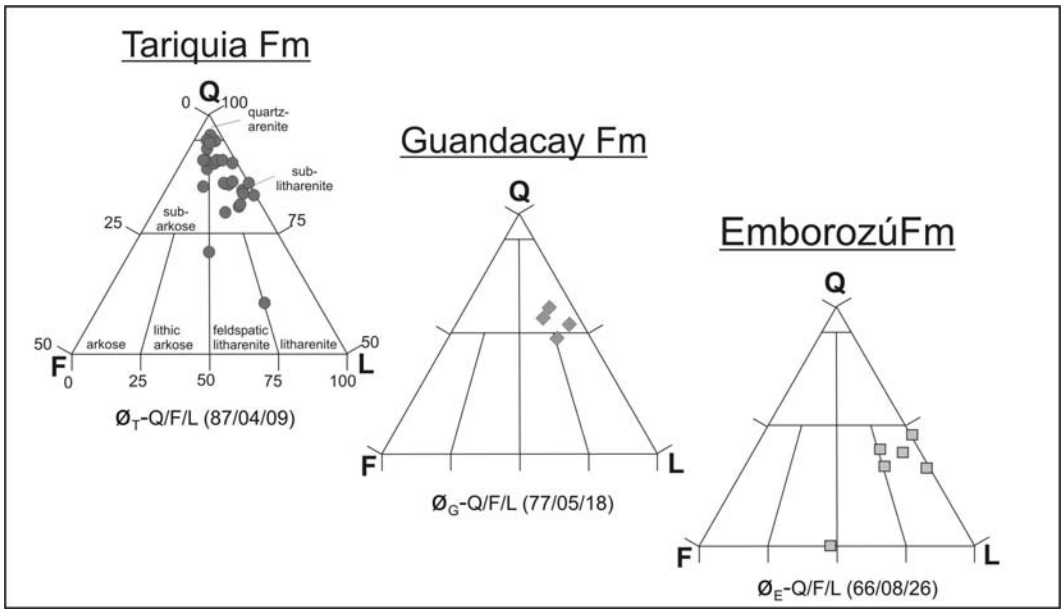


Fig. 2.10: Classification of the Tariquia-, Guandacay-, and Emborozú-sandstones.

Overall, Chaco Basin sediments are generally rich in Q, with all samples exceeding 50 % Q. All samples from the Petaca and the Yecua Formations exceed 85% Q. In the Guandacay and the Emborozú Formations, quartz content decreases (Q ≤ 80 %) mainly due to an increase of L. Sandstones of the Tariquia Formation (quartz content between 95 % and 60 %) occupy the position of a petrographic transition (Fig. 2.11).

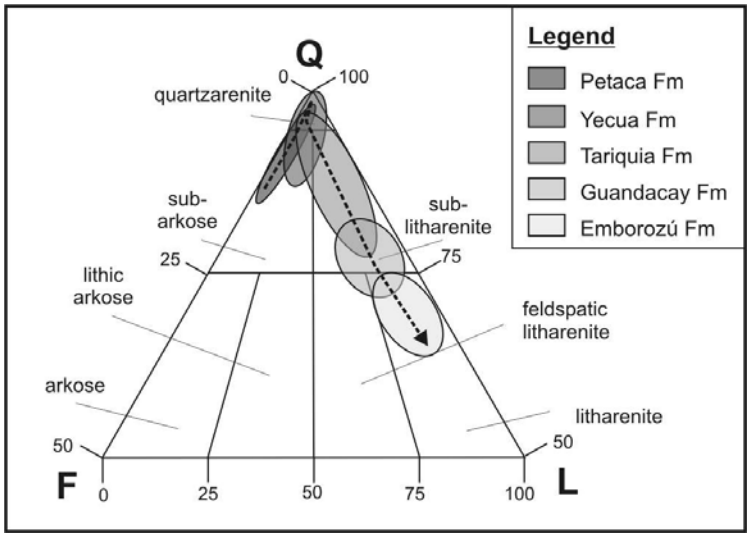


Fig. 2.11: QFL-sandstone compositional trends of the Chaco Basin fill.

# 2.5 Discussion

## 2.5.1 Provenance analysis

We used QFL, QmFLt, Qm FpFk, and QpLvLs ternary diagrams after Dickinson et al. (1985) and paleocurrent indicators to constrain provenance (Appendix A). However, the mineralogical composition of the sediments is also influenced by the size of outcrop, mineralogical maturity of the source rock, climatic conditions during transport and deposition, transport mode and distance (Blatt and Tracy, 1995).

### Petaca Formation

Samples of the Petaca Formation lie within the craton-interior block of the tectonic-provenance diagram (after Dickinson and Suczek, 1979; Fig. 2.1; Fig. 2.12). The more transport-sensitive QmFLt-diagram confirms a cratonic provenance. However, more than half of the point-counted samples fall close to the quartzose-recycled block (Fig. 2.12), indicating a high content of polycrystalline quartz.

The QmFpFk-diagram emphasizes the dominance of monocrystalline quartz compared to feldspar (Fig. 2.12). This may indicate a long transport distance, sedimentary recycling, or highly abrasive processes during transportation. The latter are dominant in aeolian environments or in high-bedload-streams (Folk, 1951; Cox and Lowe, 1995).

All these factors may have contributed to the composition of Petaca Formation. Mesozoic bedrocks underlying the Petaca Formation include dominantly aeolian Cretaceous sandstones with high quartz content (Gubbels et al., 1993). In addition, the bedload rate in the Petaca streams was likely high due to the inferred aridity (Uba et al., in revision). The low paleorelief of the Petaca Formation intensified sediment recycling from underlying material in the continental interior and likely long transport distances.

The QpLvLs-diagram confirms this interpretation with the dominance of polycrystalline quartz, minor (meta-) sedimentary lithic fragments, and the absence of volcanic lithic fragments (Fig. 2.12).

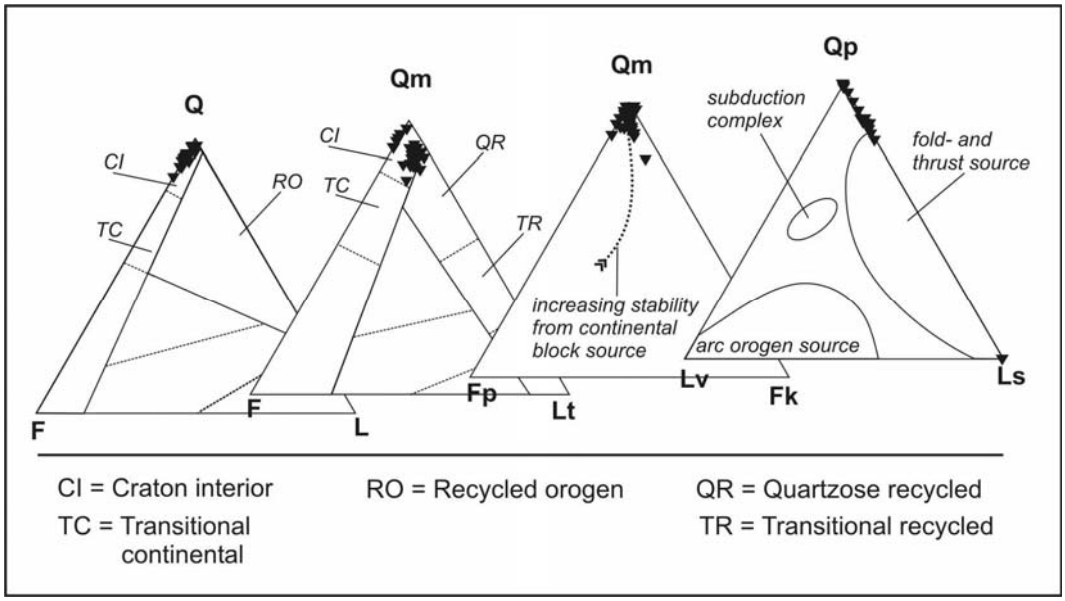


Fig. 2.12: Sandstone composition of the Petaca Formation. Framework components as in Tab. 2.1 (after Dickinson and Suczek, 1979).

## Yecua Formation

We discuss here only Yecua sandstones with a dominant extrabasinal provenance, excluding the shell-hash coquinas. These show, except for the low feldspar content, a similar petrographic composition as sandstones from the Petaca Formation and fall in the craton-interior block of the QFL- and QmFLt-diagrams (Fig. 2.13).

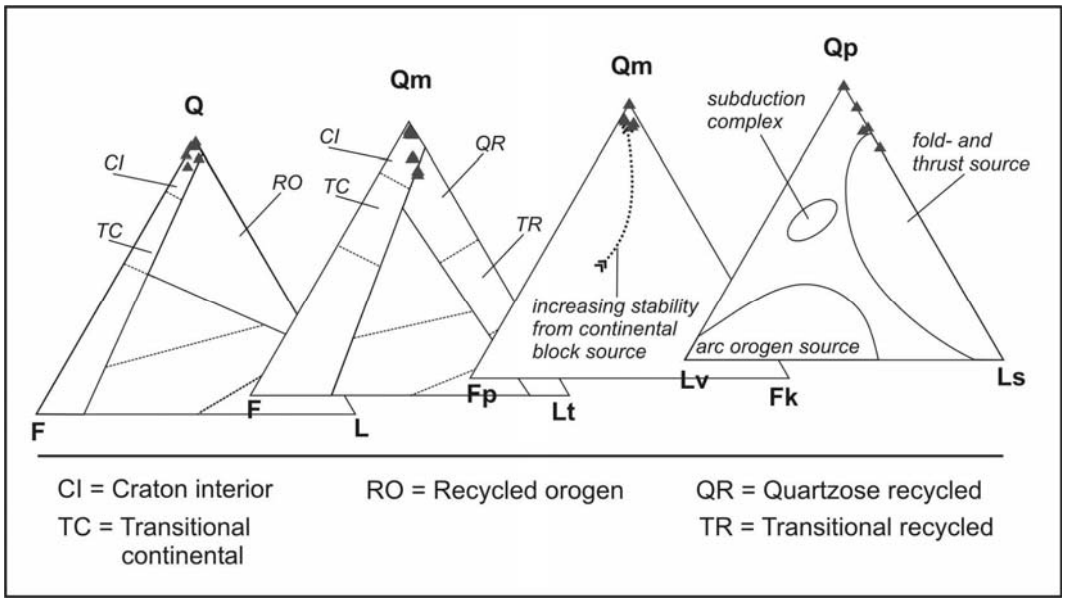


Fig. 2.13: Sandstones of the Yecua Formation. Framework components as in Tab. 2.1 (after Dickinson and Suczek, 1979).

The Qm content of the Yecua Formation is even higher than in the Petaca Formation and suggests reworking in shoreline systems. This position also suggests a dominant cratonic source rock and a low degree of influence from recycled fold-thrust belt material (Fig. 2.13).

## Tariquia Formation

Tariquia Formation sandstones appear to indicate a mixed cratonic-interior and recycled-orogen provenance (Fig. 14). However, the high Qp proportion (unlike the Qm from the underlying formations) suggests a recycled fold-thrust-belt provenance (Fig. 2.14).

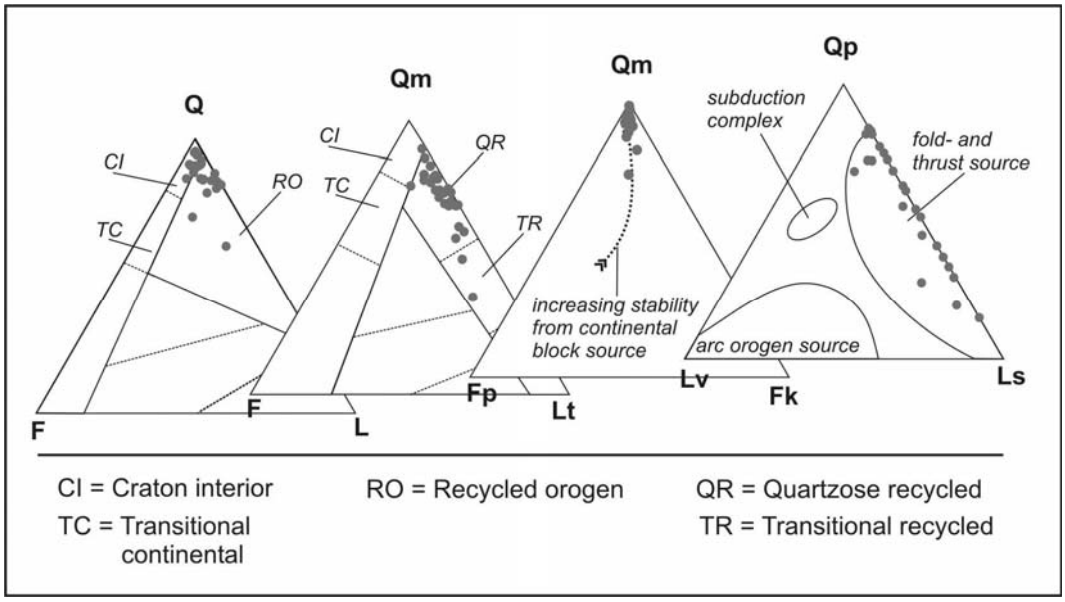


Fig. 2.14: Sandstones of the Tariquia Formation. Framework components as in Tab. 2.1 (after Dickinson and Suczek, 1979).

The high Q compared to F (Fig. 2.14) indicates a high degree of chemical weathering, a long storage in soils, or a high degree of recycling from quartzose sandstones. All these factors are also called for in the depositional setting and facies analysis of the Tariquia Formation (Uba et al., in revision).

The QpLvLs-diagram reemphasizes the importance of fold-thrust-belt sources for the Tariquia Formation with high content of polycrystalline quartz and (meta-) sedimentary lithic fragments (Fig. 2.14).

## Guandacay Formation

The four samples of the Guandacay Formation all indicate a recycled orogen provenance (Fig. 2.15) with a quartz content compared to the Tariquia Formation reduced.

The QmFLt-diagram indicates a quartzose recycled orogen provenance (Fig. 2.15).

The plagioclase and potassic feldspar content in the Guandacay Formation remains unchanged in comparison to the underlying formations (Fig. 2.15).

The increasing proportion of lithic fragments and the ratio between polycrystalline, (meta-) sedimentary, and volcanic lithic fragments defines a fold-thrust belt provenance (Fig. 2.15).

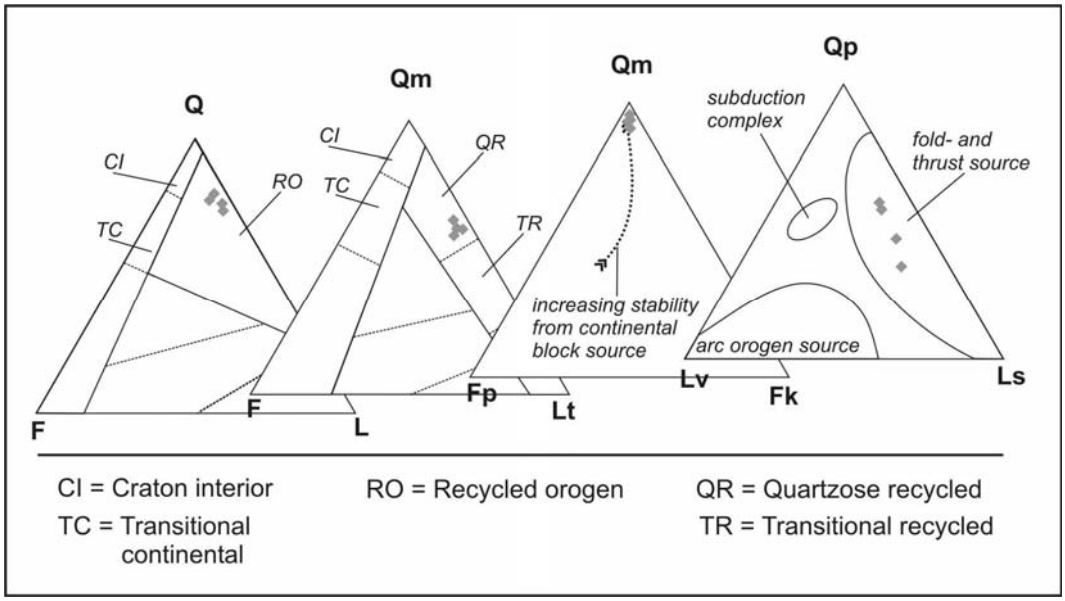


Fig. 2.15: Sandstones of the Guandacay Formation. Framework components as in Tab. 2.1 (after Dickinson and Suczek, 1979).

## Emborozú Formation

Our interpretation of Emborozú Formation provenance is limited to six samples from two sections. The QFL-diagram indicates a recycled orogen source (Fig. 2.16).

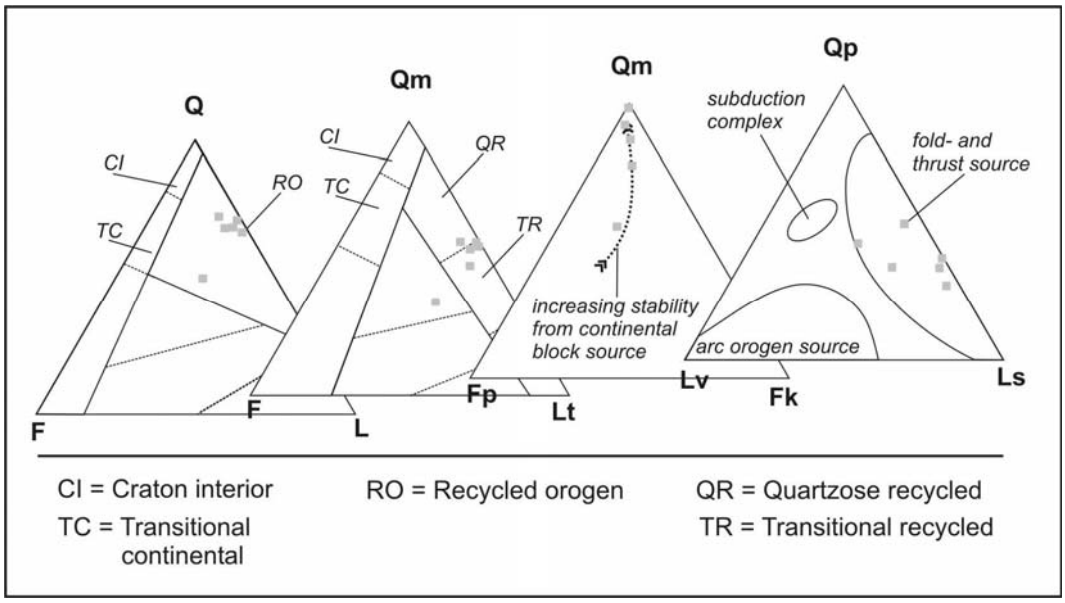


Fig. 2.16: Sandstones of the Emborozú Formation. Framework components as in Tab. 2.1 (after Dickinson and Suczek, 1979).

Similar to the composition of the underlying Guandacay Formation, the QmFLt-diagram suggests a quartzose– to transitional-recycled provenance, except one sample that represents a composition typical of a dissected magmatic arc source (Fig. 2.16). Possibly, reworked tuffaceous components contributed to this composition. In addition, a tuff bed occurred just below the sample site.

The QmFpFk-diagram illustrates a reduced Qm content with respect to the underlying formations, possibly reflecting a decreasing transportation distance and higher survivability of

Lv and Qp grains. All these observations fit well with sedimentary observations in the Emborozú Formation and its depositional interpretation of a proximal alluvial fan.

The QpLvLs-diagram indicates a mix of a fold-thrust belt source with a volcanic component within the dissected magmatic arc provenance (Fig. 2.16).

### Trends in sandstone composition

The sandstone composition of the Cenozoic formations, plotted in the QFL- and QmFLt-diagrams, show a trend from mainly craton-interior continental source rock (Petaca and Yecua Formations) to recycled orogen sources of the Tariquia, Guandacay and Emborozú Formations (Fig. 2.17). However, the Yecua Formation shows reduced feldspar and increased lithic components, which we interpret as a minor influence of recycled orogen sources (see QmFLt-diagram in Fig. 2.17).

The QmFpFk-diagram illustrates the dominance of continental influence throughout the Cenozoic strata by increasing influence of feldspar compared to monocrystalline quartz from the Petaca toward the Emborozú Formation.

Comparative studies of the lithic components show that the Petaca and the Yecua Formations contain mainly Qp-components. The overlying formations, in contrast, show a decreasing influence of Qp and are clearly represented in the fold-thrust source provenance area. Even so, volcanic lithic components remain low throughout the foreland basin fill.

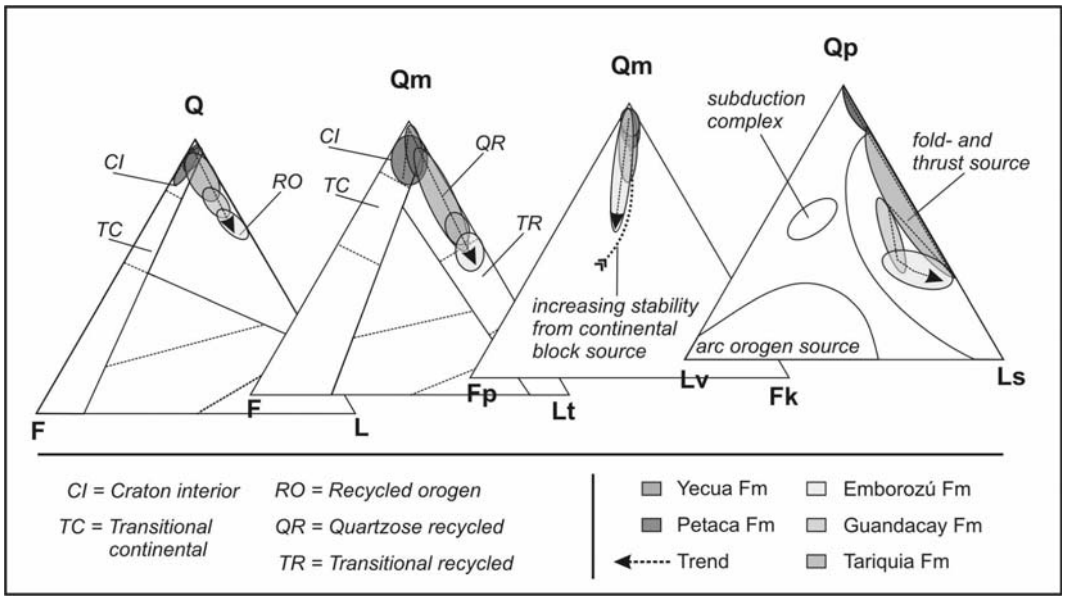


Fig. 2.17: Ternary diagrams showing modal composition of the five Cenozoic formations (after Dickinson and Suczek, 1979).

## 2.5.2 Maturity

Textural and mineralogical maturity follow consistent trends in the Chaco foreland basin fill and collectively suggest that factors contributing to high maturity lose relative importance through time. Textural maturity of sandstone after Folk (1951) is defined by clay content, the degree of sorting, and degree of rounding (Fig. 2.18).

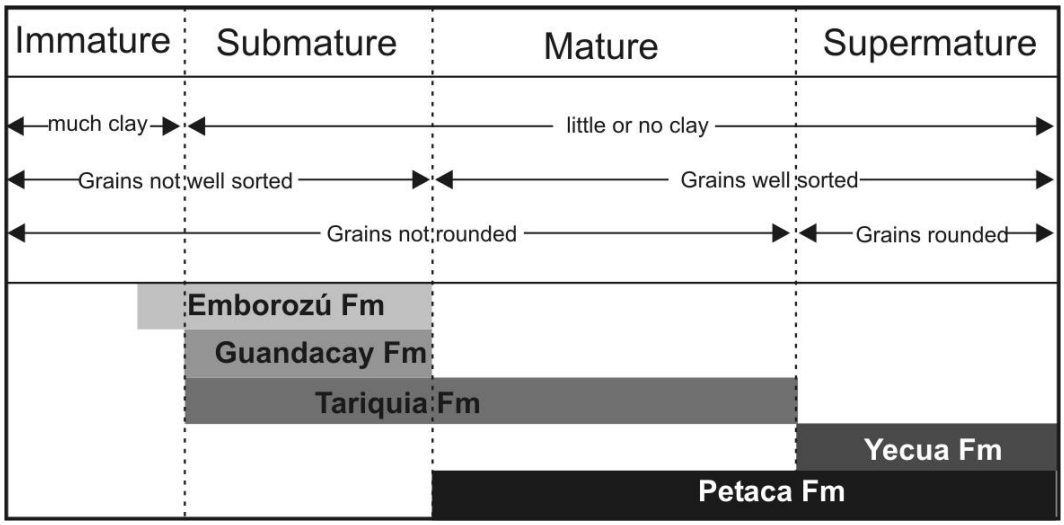


Fig. 2.18: Textural maturity of sands after Folk (1951).

The mineralogical maturity can be expressed quantitatively by the maturity index, defined by the ratio between silicate grains (monocrystalline and polycrystalline quartz as well as cherts) and the sum of feldspar and lithic fragments (Tab. 2.2). This method has the potential to identify alteration processes of the source rocks, which lead to enrichment of stable components (such as quartz) relative to instable components (such as feldspar). Another index of maturity is the ratio between the polycrystalline and the monocrystalline quartz. This ratio considers the mechanical instability of Qp with respect to Qm (Tab. 2.2).

Tab. 2.2: Maturity index and Qp/Qm-ratio of the Cenozoic formations in the northern part of the Chaco Basin

| Formation | Number of samples | Maturity Index | Qp/Qm-ratio |
|---|---|---|---|
| Emborozú | 6 | 1.94 | 0.44 |
| Guandacay | 4 | 3.38 | 0.28 |
| Tariquia | 25 | 6.64 | 0.17 |
| Yecua | 7 | 20.88 | 0.07 |
| Petaca | 30 | 14.50 | 0.09 |

Tab. 2.2 indicates quantitatively an overall decreasing maturity index with time. Only the Yecua value does not conform to this trend, probably due to the high degree of reworking in its shoreline systems.

### 2.5.3 Climate condition

The Oligocene climate in the study area (represented by deposits of the Petaca Formation) is thought to have been arid or semiarid due to the occurrence of calcrete paleosols and small aeolian dune complexes. Remobilized gypsum in sediments of the Yecua Formation (Middle Miocene) also may indicate semiaridity, supported by Yecua ostracodes adapted to hypersalinity (Hulka et al., in press; chapter 3).

Uba et al. (in revision) inferred climatic change towards increased humidity, starting in the latest Tariquia time because of increasing appearance of root traces and thin coal seams, and a concomitant decrease in calcrete, mudcrack, and rip-up clast abundance. Climate conditions of the Guandacay and Emborozú Formations also influence the abundance of feldspar- and lithic fraction.

The present climate of the Chaco Basin represents a semihumid to semiarid climate, suggesting that climatically induced alteration processes are not relevant for the youngest deposits. The increasing feldspar- and lithic fraction since the Late Miocene (Guandacay and Emborozú Formations) may therefore also reflect increased transport efficiency in streams combined with a reduced transport distance, outweighing the effects of increased chemical weathering related to climate change.

## 2.6 Conclusions

Provenance analysis of the Petaca Formation indicates a cratonic-interior provenance with high degree of mineralogical and tectonical maturity (Fig. 2.18). Reworked paleosols represent a high degree of sedimentary recycling and short transportation distances in an arid to semihumid climate.

Yecua Formation sandstones indicate a cratonic interior source and minor influence of a quartzose recycled orogen provenance, also indicated by extensive shoreline systems prone to sedimentary recycling and isotopic fingerprinting indicating cratonic-derived water.

Tariquia Formation sandstones mark a pronounced change in provenance and show a high contribution from fold-thrust belt source rocks, masking a still significant craton-interior provenance. These may result from recycling of the underlying older formations (Yecua Formation, Petaca Formation, or Cretaceous aeolian sandstones) or the exposure of Mesozoic strata in the rising Subandean Belt, deposited in a medium-distal foredeep position within the deepening retroarc foreland basin.

The decreasing-quartz trend in the Tariquia, Guandacay and Emborozú Formations is likely a function of increasing stream power, aided by shorter transportation distances, and resulting in an increasing feldspar and lithic proportion.

## Acknowledgments

This research project represents part of the senior author's Ph.D. thesis and was supported by the SFB 267 and Chaco S.A., Santa Cruz, Bolivia. We thank Oscar Araníbar, Fernando Alegría, and Nigel Robinson of Chaco S.A. for financial and logistic assistance, and D. Mertmann and E. Scheuber for critical comments and help on an early version of the manuscript.